JACS
JOURNAL OF THE AMERICAN CHEMICAL SOCIETY

Article

pubs.acs.org/JACS

Graphene Oxide/Nucleic-Acid-Stabilized Silver Nanoclusters: Functional Hybrid Materials for Optical Aptamer Sensing and Multiplexed Analysis of Pathogenic DNAs

Xiaoqing Liu, Fuan Wang, Ruth Aizen, Omer Yehezkeli, and Itamar Willner*

Institute of Chemistry, Center for Nanoscience and Nanotechnology, The Hebrew University of Jerusalem, Jerusalem 91904, Israel

Supporting Information

ABSTRACT: Hybrid systems consisting of nucleic-acid-functionalized silver nanoclusters (AgNCs) and graphene oxide (GO) are used for the development of fluorescent DNA sensors and aptasensors, and for the multiplexed analysis of a series of genes of infectious pathogens. Two types of nucleic-acid-stabilized AgNCs are used: one type includes the red-emitting AgNCs (616 nm) and the second type is near-infrared-emitting AgNCs (775 nm). Whereas the nucleic-acid-stabilized AgNCs do not bind to GO, the conjugation of single-stranded nucleic acid to the DNA-stabilized AgNCs leads to the adsorption of the hybrid nanostructures to GO and to the fluorescence quenching of the AgNCs. By the conjugation of oligonucleotide sequences acting as probes for target genes, or as aptamer sequences, to the nucleic-acid-protected AgNCs, the desorption of the probe/nucleic-acid-stabilized AgNCs from GO through the formation of duplex DNA structures or aptamer–substrate complexes leads to the generation of fluorescence as a readout signal for the sensing events. The hybrid nanostructures are implemented for the analysis of hepatitis B virus gene (HBV), the immunodeficiency virus gene (HIV), and the syphilis (*Treponema pallidum*) gene. Multiplexed analysis of the genes is demonstrated. The nucleic-acid-AgNCs-modified GO is also applied to detect ATP or thrombin through the release of the respective AgNCs-labeled aptamer–substrate complexes from GO.

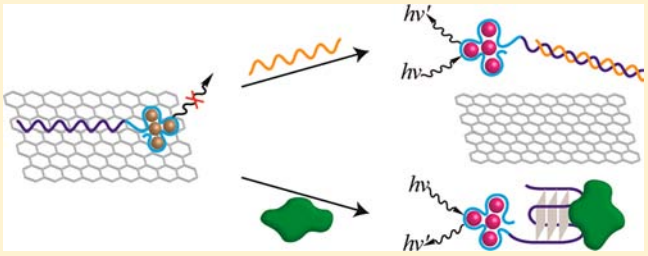

INTRODUCTION

The synthesis and application of fluorescent metallic nanoclusters, especially nucleic-acid-stabilized silver nanoclusters (AgNCs/DNA) attract substantial research interest.[1] Cytosine-rich nucleic acids usually act as stabilizing template for AgNCs.[2] The AgNCs consist of a few silver atoms and exhibit interesting photophysical properties. The AgNCs reveal high luminescence quantum yields, tunable emissions, controlled by the size and the protecting layer of the nanoclusters, good photostability, water solubility, biocompatibility and low toxicity. These features turn the AgNCs to attractive materials for optical sensing and biological imaging applications.[3] Indeed, AgNCs/DNA have been applied as fluorescent labels for sensing of metal ions such as Hg^{2+} or Cu^{2+},[4] bioactive thiols such as cysteine, homocysteine or glutathione,[5] probing enzyme activities such as tyrosinase or glucose oxidase,[6] detection of aptamer–substrate recognition complexes[7] such as detection of thrombin or ATP, and analysis of single nucleotide mutation in DNA[8] or microRNAs (miRNAs).[9] AgNCs/DNA conjugates were also used for cell imaging.[10]

Graphene oxide, GO, is an interesting nanomaterial for sensing applications.[11] It was found that, whereas single-stranded nucleic acids bind to the surface of GO through π–π stacking interactions between the hexagonal graphitic units of GO and the nucleotides, the hybridization of the single-stranded DNA with the complementary nucleic acid yields a duplex that lacks affinity toward GO.[12] Since fluorophores adsorbed on GO are effectively quenched by electron transfer or energy transfer mechanisms, and realizing the adsorption/desorption properties of single-strand/duplex DNAs to and from GO, respectively, fluorophore-labeled nucleic acids and GO were implemented to develop different optical biosensors.[13] For example, fluorophore-labeled nucleic acid probes adsorbed onto GO were desorbed from the GO matrix by the target-induced formation of a duplex DNA.[14] Similarly, fluorophore-labeled aptamers were desorbed from GO while triggering-on the fluorescence as readout signal.[14] Also, amplification routes for the detection of DNA analytes in the presence of GO matrices were developed. For example, by the exonuclease III, Exo III, digestion of the desorbed duplex from GO, the target DNA could be regenerated, thus leading to the cyclic desorption of the fluorescent probe from the GO matrix.[15]

In the present study, we report on the integration of AgNCs/DNA with GO, and the implementation of these hybrid materials for the development of DNA sensors and aptasensors. We specifically apply the tunable fluorescence properties of AgNCs to demonstrate the multiplexed analysis of DNAs of infectious pathogens. We also apply the nucleic-acid-functionalized AgNCs/GO to assay aptamer–substrate complexes of ATP and thrombin. In contrast to related GO-based DNA sensors or aptasensors that have implemented the desorption of

Received: April 8, 2013
Published: July 10, 2013

   dx.doi.org/10.1021/ja403485r | J. Am. Chem. Soc. 2013, 135, 11832–11839

fluorophore-modified nucleic acid probes from GO,[13−15] the present study allows the simple tethering of the specific oligonucleotides stabilizing the AgNCs to the nucleic acid probes. As a result, the AgNCs fluorescent labels can be easily prepared prior to the deposition on GO. In addition, the resulting nucleic-acid-protected AgNCs revealed high stability and photostability.

EXPERIMENTAL METHODS

Materials. $AgNO_3$, $NaBH_4$, $NaNO_3$, KNO_3, graphite powder, thrombin, bovine serum albumin (BSA), adenosine 5′-triphosphate (ATP), uridine 5′-triphosphate (UTP), guanosine 5′-triphosphate (GTP), and guanosine 5′-monophosphate (GMP) were purchased from Sigma-Aldrich. Ultrapure water from a NANOpure Diamond (Barnstead Int., Dubuque, IA) source was used throughout the experiments.

All oligonucleotides were purchased from Integrated DNA Technologies, Inc. (Coralville, IA). The nucleic acids were HPLC-purified and freeze-dried. Stock solutions of 100 μM of DNA were prepared with 10 mM phosphate buffer, pH 7.4.

The sequences of the oligonucleotides are provided.

Instrument. Fluorescence measurements were carried out using a Cary Eclipse Fluorimeter (Varian, Inc.). The red-emitting AgNCs were excited at λ = 530 nm. The near-infrared-emitting AgNCs were excited at λ = 730 nm.

Preparation of Graphene Oxide. Graphene Oxide was prepared according to Hummers' method, and similar to a previously reported protocol.[15,19] The product was diluted and sonicated for 1 h to separate any aggregated graphite oxide layers and further centrifuged to remove any graphite oxide residue prior to use.

Synthesis of DNA-Stabilized AgNCs. The method followed the reported protocol.[2] The AgNCs were synthesized by mixing $AgNO_3$ with the DNA solution and adding $NaBH_4$ while shaking. Typically, 15 μL of the DNA template (100 μM) for the red-emitting AgNCs was mixed with 73 μL of phosphate buffer (20 mM, pH 7.0). To this solution, freshly prepared 6 μL of $AgNO_3$ aqueous solution (1.5 mM) was added, followed by the vigorous shaking of the solution for 30 s. After 15 min, freshly prepared 6 μL of $NaBH_4$ aqueous solution (1.5 mM) was added to the solution, followed by vigorous shaking of the mixture for 30 s. The synthesis of the near-infrared-emitting AgNCs was similar to that of the red-emitting AgNCs, except that final concentrations of 240 μM $AgNO_3$ and 120 μM $NaBH_4$ were used. The solutions were kept in the dark at room temperature and allowed to react for 12 h.

Analysis of Target DNA, ATP, and Thrombin Using the Fluorescent Nucleic-Acid-Protected AgNCs as Labels. *Analysis of DNA Targets.* The analyses were performed in a reaction volume of 150 μL phosphate buffer (10 mM, pH 7.0) that included 200 mM $NaNO_3$. For the systems applying the red-emitting, nucleic-acid-functionalized AgNCs as probe, 0.025 mg/mL of GO and 100 nM of the red-emitting, nucleic-acid-functionalized AgNCs were added to the reaction volume. For the systems applying the near-infrared-emitting AgNCs as probes, 0.02 mg/mL of GO and 100 nM of the nucleic-acid-functionalized AgNCs were added to the respective volume. The systems were incubated until the fluorescence of the AgNCs in the respective reaction mixture was quenched. The respective DNA targets were then added to the respective reaction mixture, and the fluorescence of the desorbed AgNCs were measured. For the multiplexed analysis of pathogen DNA, GO, the red-emitting AgNCs-linked DNA, and the near-infrared-emitting AgNCs-linked DNA were mixed together. The respective target DNAs were then added, and the time-dependent fluorescence changes of the AgNCs were recorded. For the multiplexed analysis of the HBV gene (400 nM) and of the HIV gene (400 nM), probe **7** (50 nM) and probe **10** (75 nM), and 0.04 mg/mL of GO were used. For the multiplexed analysis of the syphilis gene (250 nM) and of the HBV gene (500 nM), probe **12** (100 nM) and probe **10** (100 nM), and 0.07 mg/mL of GO were used.

ATP or Thrombin Assays. The reaction mixture consisted of 150 μL of 10 mM phosphate buffer (pH 7.0) that included $NaNO_3$ (200 mM) and KNO_3 (50 mM). The AgNCs-linked thrombin aptamer or the AgNCs-linked ATP aptamer (100 nM) was mixed with 0.025 mg/mL of GO in the reaction volume, and different concentrations of thrombin or ATP were added to the respective system. The fluorescence resulting upon the formation of the respective aptamer−substrate complexes and their desorption from GO were monitored.

(**1**) 5′-ACCCGAACCTGGGCTACCACCCTTAATCCCC-3′ (I)

(**2**) 5′-CCCACCCACCCTCCCA-3′ (I)

(**3**) 5′-ACCCGAACCTGGGCTACCACCCTTAATCCCC AATCCGTCGAGCAGAGTT-3′ (I; II)

(**4**) 5′-AACTCTGCTCGACGGATT-3′

(**4a**) 5′-AACTCTGCTAGACGGATT-3′

(**5**) 5′-AGTTACTCTCTTTTTTGCCTTCTGA-3′

(**5a**) 5′-AGTTACTCTCTTTATTGCCTTCTGA-3′

(**5b**) 5′-AGTTACTATCTTTTTTGACTTCTGA-3′

(**6**) 5′-ACCCGAACCTGGGCTACCACCCTTAATCCCC TCAGAAGGCAAAAAAGAGAGTAACT-3′ (I; II)

(**7**) 5′-ACCCGAACCTGGGCTACCACCCTTAATCCCC GAGACCATCAATGAGGAAGCTGCAGAATGGGAT-3′ (I; II)

(**8**) 5′-ATCCCATTCTGCAGCTTCCTCATTGATGGTCTC-3′

(**9**) 5′-CCCACCCACCCTCCCA GAGACCATCAATGAGGAAGCTGCAGAATGGGAT-3′ (I; II)

(**10**) 5′-CCCACCCACCCTCCCA TCAGAAGGCAAAAAAGAGAGTAACT-3′ (I; II)

(**11**) 5′-ACTATCCTCAGTGAGCATTGTC-3′

(**12**) 5′-ACCCGAACCTGGGCTACCACCCTTAATCCCC GACAATGCTCACTGAGGATAGT-3′ (I; II)

(**13**) 5′-TACCTGGGGGAGTATTGCGGAGGAAGGTA ACCCGAACCTGGGCTACCACCCTTAATCCCC-3′ (III; I)

(**14**) 5′-CCCACCCACCCTCCCA TACCTGGGGGAGTATTGCGGAGGAAGGTA-3′ (I; III)

(**15**) 5′-GGTTGGTGTGGTTGGAT ACCCGAACCTGGGCTACCACCCTTAATCCCC-3′ (IV; I)

(**16**) 5′-GGTTGGTGTGGTTGG ACCCGAACCTGGGCTACCACCCTTAATCCCC-3′ (IV; I)

RESULTS AND DISCUSSION

Two different AgNCs were applied in the present study. Type I of red-emitting AgNCs are stabilized by the nucleic acid sequence **1**, and they exhibit fluorescence at λ = 616 nm. Type II of near-infrared-emitting AgNCs are stabilized by the nucleic

dx.doi.org/10.1021/ja403485r | J. Am. Chem. Soc. 2013, 135, 11832−11839

acid sequence **2**, and they reveal fluorescence at λ = 775 nm. The excitation and emission spectra of the two types of AgNCs are presented in Figure S1, Supporting Information. Even though the AgNCs-protecting nucleic acid sequences **1** and **2** are single strands, the resulting AgNCs/DNA-**1** or -**2** complexes reveal low affinity for GO, and the luminescence of the AgNCs is inefficiently quenched (less than 10%). This suggests that the interactions of the bases stabilizing the AgNCs perturb their association to GO, thus eliminating the binding of the protected AgNCs to the GO. The analytical platform for sensing a target DNA by a AgNCs-functionalized probe is exemplified in Scheme 1. The nucleic acid sequence protecting

Scheme 1. Assay of the Target DNAs Using DNA-Templated AgNCs/GO Hybrids as Sensing Matrices

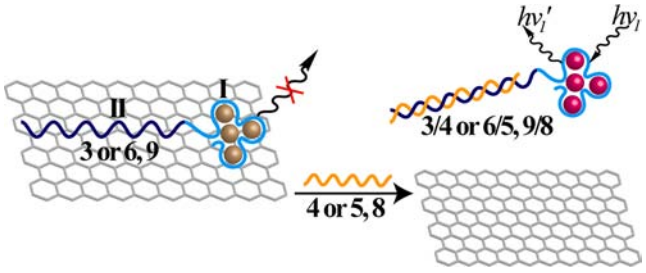

the AgNCs (domain I) is elongated with the nucleic acid probe sequence (domain II) that is complementary to the target analyte. For example, the nucleic acid **3** includes in its domain II the sequence complementary to the analyte **4**. Adsorption of the AgNCs-functionalized **3** to GO results in the quenching of the luminescence of the AgNCs, see Figure S2, Supporting Information. Formation of the duplex between **4** and **3** results in the desorption of the structure **3**/**4**, leading to the regeneration of fluorescence. As the desorption of probe **3** from GO is controlled by the concentration of the target DNA (**4**), the method is anticipated to provide a quantitative means to analyze the target. The suggested analytical platform raises some basic issues that need to be addressed: (a) Are the desorbed nucleic-acid-stabilized AgNCs stable? (b) What is the time-course for desorption of the resulting probe/AgNCs/analyte from GO? (c) What is the sensitivity/specificity and possible applicability of the analytical platform? To address these issues, we examined the analysis of a random DNA sequence (**4**), using **3**−AgNCs adsorbed onto GO, as a model system. We then implemented the sensing platform to analyze the hepatitis B virus (HBV) gene, the human immunodeficiency virus (HIV) gene, and the syphilis (*Treponema pallidum*) gene. The characterization of the fundamental analytical features for the detection of the random sequence (**4**) by the 616 nm-emitting AgNCs-modified probe **3** associated with GO is presented in Figure S3, in the Supporting Information. In Figure S3A, the time-dependent fluorescence changes in the solution, upon subjecting the **3**-functionalized GO to the analyte (**4**), are presented. The fluorescence increases with time, implying that the AgNCs-modified probe **3** is, indeed, desorbed from the GO. The fluorescence reaches a saturation value after ca. 80 min, suggesting that this is the optimal time-interval to follow the desorption of **3** from GO. Nonetheless, one should note that after ca. 40 min the fluorescence of the desorbed AgNCs−**3**/**4** duplex corresponds to ca. 80% of the saturated fluorescence value, suggesting that the sensing time-interval may be shortened, while losing some of the sensitivity. In fact, we find that the desorption time-interval is controlled by the stabilizing energy of the desorbed duplex structure, and thus, for the desorption of the viral genes, shorter desorption times may be used due to the enhanced stabilities of the resulting desorbed duplexes (vide infra for detailed discussion). Figure S3B shows the fluorescence spectra resulting upon the interaction of the **3**−AgNCs/GO hybrid with different concentrations of analyte **4** for a fixed time-interval of 80 min. As the concentration of the complementary nucleic acid **4** increases, the luminescence signals of the released red-emitting AgNCs-labeled probe **3** are intensified. The target DNA (**4**) could be analyzed with a detection limit of 1 nM (for the respective calibration curve and evaluation of the selectivity of the system to analyze mutants see Figure S3B,C, Supporting Information).

Realizing that GO modified with probe nucleic acids labeled with the AgNCs acts as hybrid nanomaterial for the optical detection of DNA, this sensing platform was implemented to detect a series of medically significant genes, while applying two types of the GO/AgNCs systems (red and near-infrared emitters). The genes that were analyzed include the HBV gene, HIV gene, and the syphilis gene. For the analysis of the HBV gene (**5**) the nucleic acid **6**−AgNCs acts as functional optical probe, according to Scheme 1. It includes the domain II, complementary to the target HBV gene, and this is conjugated to the AgNCs/nucleic acid label emitting at 616 nm. Figure 1A shows the time-dependent luminescence changes and the respective calibration curve (inset) upon analyzing **5** (100 nM) through the target-induced desorption of **6**−AgNCs from the GO matrix. Figure 1B depicts the fluorescence spectra of the desorbed AgNCs upon analyzing different concentrations of **5** for a fixed time interval of 80 min and the corresponding calibration curve, Figure 1B, inset. As the concentration of the HBV gene increases, the resulting fluorescence is intensified. The method allowed the analysis of the HBV gene with a detection limit of 0.5 nM. Control experiments revealed that, in the absence of GO, the addition of the nucleic acid **5** to **6**−AgNCs did not lead to any fluorescence changes of the AgNCs (see Figure S4, Supporting Information). (For the analysis of one- and two-base mutations at the HBV gene and the complementary stringency control experiments, see Figure S5 and Table S1, Supporting Information.) For the use of **7** functionalized with the red-emitting AgNCs, to analyze the HIV gene (**8**), see Figure S6, Supporting Information.

Similarly, the near-infrared-emitting AgNCs stabilized by the nucleic acid, and emitting at 775 nm, were used as optical labels for sensing the genes. This is exemplified with the analysis of the HIV gene, according to Scheme 1. The nucleic acid **9** that includes the domain II, complementary to the HIV gene, and is conjugated to the nucleic acid sequence (domain I) that stabilizes AgNCs emitting at 775 nm, was adsorbed onto GO. Figure 2A shows the time-dependent fluorescence changes upon analyzing the HIV gene (**8**), by the **9**−AgNCs-functionalized GO matrix. In the presence of **8**, a time-dependent increase in the fluorescence of the solution is observed, consistent with the desorption of the **9**−AgNCs from the GO as a result of the formation of the **9**/**8** duplex structure. Figure 2B depicts the fluorescence spectra of the AgNCs upon analyzing different concentrations of the HIV gene (**8**), by the **9**−AgNCs/GO hybrid matrix, and the resulting calibration curve, Figure 2B, inset. The system enabled the analysis of the HIV gene with a detection limit of 1 nM. (In analogy, the HBV gene was also analyzed by the 775 nm-emitting, **10**-stabilized AgNCs, see Figure S7, Supporting Information.) For the optimized conditions of the synthesis of the

dx.doi.org/10.1021/ja403485r | J. Am. Chem. Soc. 2013, 135, 11832−11839

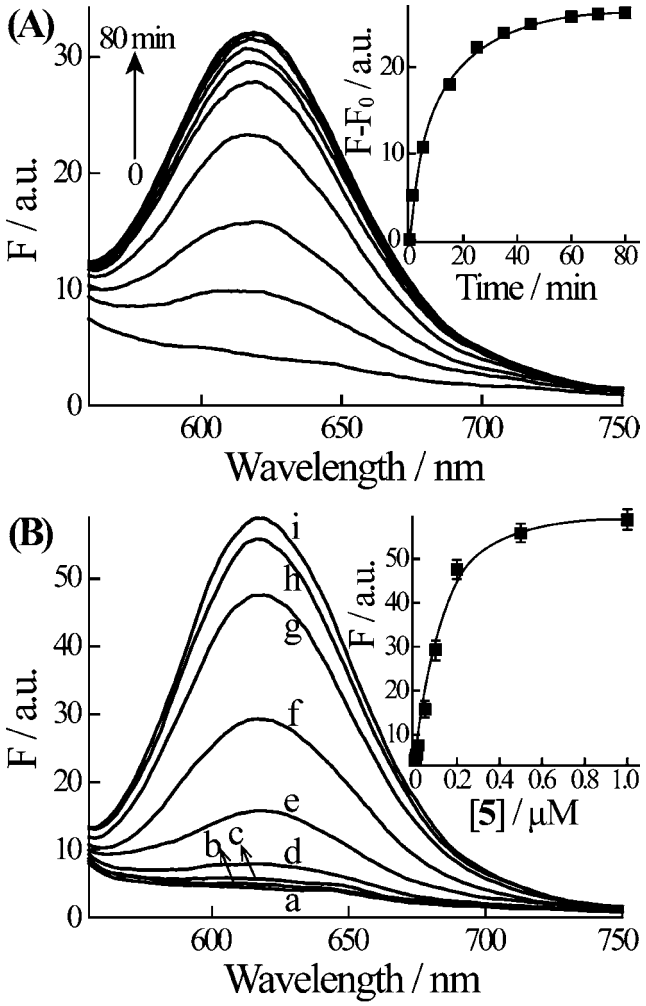

Figure 1. (A) Time-dependent fluorescence spectra of the red-emitting AgNCs upon challenging the **6**–AgNCs/GO with the HBV target gene (**5**) (100 nM). Inset: time-dependent fluorescence changes at λ = 616 nm upon analyzing **5** by the **6**–AgNCs/GO. (B) Fluorescence spectra of the AgNCs upon analyzing different concentrations of the HBV gene (**5**) by the **6**–AgNCs/GO system: (a) 0, (b) 2 nM, (c)10 nM, (d) 20 nM, (e)50 nM, (f) 100 nM, (g) 200 nM, (h) 500 nM, and (i) 1000 nM. Fluorescence spectra were recorded after a fixed time interval of 80 min. Inset: calibration curve corresponding to the luminescence of the related AgNCs (at λ = 616 nm) in the presence of different concentrations of **5**. F_0 and F correspond to the fluorescence of the system in the absence and presence of target DNA, respectively. Error bars were derived from N = 3 experiments.

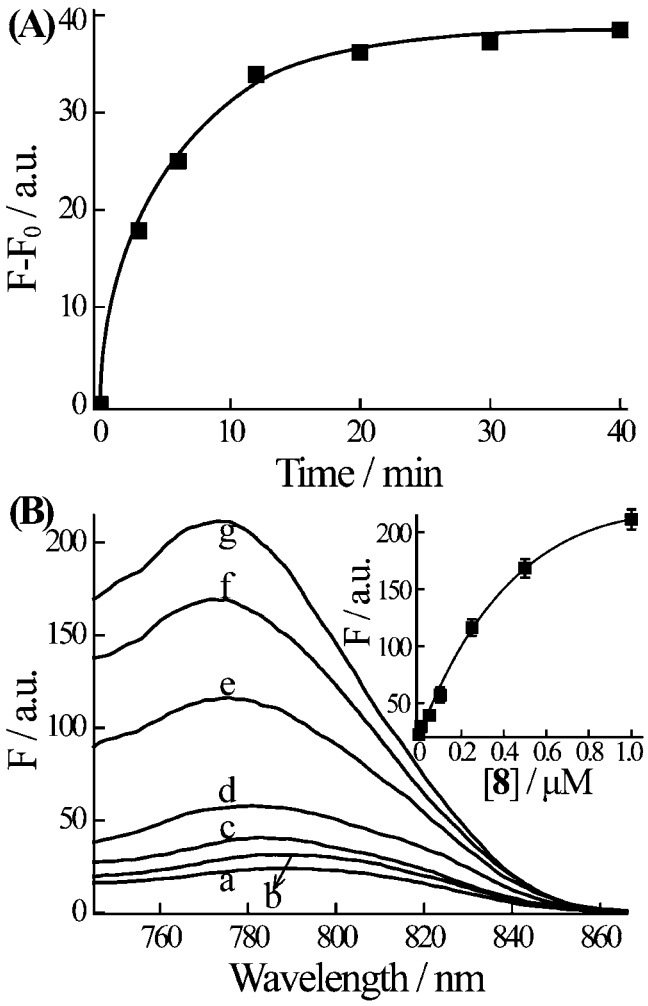

Figure 2. (A) Time-dependent fluorescence changes of the near-infrared-emitting AgNCs at λ = 775 nm upon challenging the **9**–AgNCs/GO hybrid with the HIV gene **8** (100 nM). (B) Fluorescence spectra of the AgNCs upon analyzing different concentrations of the HIV target gene **8** by the **9**–AgNCs/GO system: (a) 0, (b) 10 nM, (c) 50 nM, (d) 100 nM, (e) 250 nM, (f) 500 nM, and (g) 1000 nM. Inset: calibration curve corresponding to the fluorescence signal (at λ = 775 nm) at different concentrations of **8**. Fluorescence spectra were recorded after a fixed time interval of 60 min. F_0 and F correspond to the fluorescence of the system in the absence and presence of target DNA, respectively. Error bars were derived from N = 4 experiments.

fluorescent **9**–AgNCs and the **10**–AgNCs, see Figure S8, Supporting Information.

The time-dependent release of the nucleic acid probes by the respective targets controls the analysis time-interval, and it is an important parameter that characterizes the sensor's performance. From the results presented in Figure S3A, one many conclude that the time interval for reaching saturation for releasing the random sequence **4** (100 nM) was ca. 80 min. In turn, the time interval for reaching the saturated release of the AgNCs (616 nm)–**5**/**6** and of AgNCs (775 nm)–**8**/**9** also at a target concentration of 100 nM, corresponds to ca. 50 and ca. 25 min, respectively. A possible origin for the different rates of releasing the different probe/target complexes could be the relative stabilities of the resulting desorbed duplex structures. The estimated free-energy values associated with the formation of the duplexes **3**/**4**, **5**/**6**, and **8**/**9** correspond to −34.5, −43.3, and −62.3 kcal·mol^{-1}, respectively. Thus, the stability of the desorbed duplexes correlates with the rate of their release from GO.

The availability of two different luminescent AgNCs optical probes that can be selectively desorbed from GO suggests that the multiplexed analysis of two targets could be feasible. Multiplexed optical DNA sensing is a challenging topic in bioanalysis, and different optical labels, such as different fluorophores,[15,16] different sized quantum dots[17] or metal barcodes,[18] were used for multiplexed analysis of DNA or aptamer–substrate complexes. Scheme 2 schematically depicts the multiplexed analysis of the HBV gene (**5**) and of the HIV gene (**8**), using the 775 nm-luminescent AgNCs probe **10**, complementary to the HBV gene, and the 616 nm-luminescent AgNCs probe **7**, complementary to the HIV gene. The two probes (**10** and **7**) were adsorbed onto the GO. Selective desorption of **10** or **7** is anticipated to proceed in the presence

dx.doi.org/10.1021/ja403485r | J. Am. Chem. Soc. 2013, 135, 11832–11839

Scheme 2. Multiplexed Analysis of the HBV Gene (5) and of the HIV Gene (8) Using the Near-Infrared- and Red-Emitting AgNCs Probes

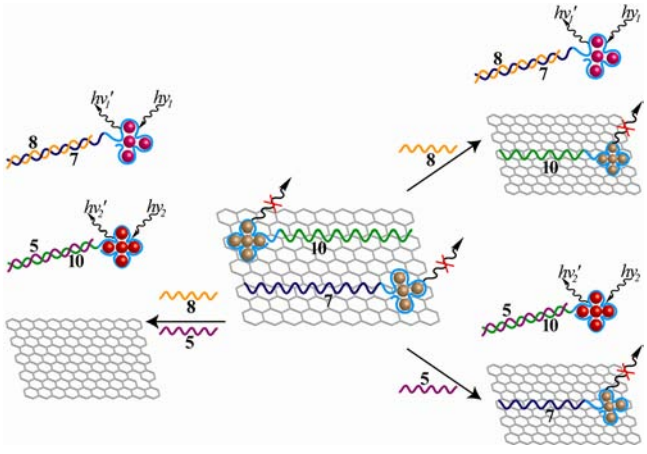

of the HBV and HIV genes, respectively, whereas desorption of the two genes, and the activation of the luminescence properties of the two AgNCs, is expected upon challenging the functionalized GO surface with the two genes. Figure 3 demonstrates the multiplexed analysis of the two genes by the **10** and 7−functionalized GO. Whereas very weak luminescence is detected in the absence of the genes, Figure 3A, the treatment of the modified GO with the HBV gene (**5**) or the HIV gene (**8**) triggers the luminescence of the 775 nm or of the 616 nm AgNCs probes as a result of the selective desorption of the two genes, Figure 3, panels B or C, respectively. Challenging of the **10**- and 7-functionalized GO with the two genes leads to the desorption of the two probes from the GO surface and to the generation of the fluorescence characteristic to the two probes, Figure 3D. By a similar approach, the multiplexed analysis of the HBV gene (**5**) and of the syphilis gene (**11**) was demonstrated. In these experiments, the 616 nm-luminescent probe **12** was used to analyze the syphilis gene (**11**), whereas the near-infrared-luminescent probe **10** was applied to detect the HBV gene (**5**), see Figure S9, Supporting Information.

The luminescent AgNCs were further used for analyzing aptamer−substrate complexes. The method to analyze ATP by the respective aptamer complex is displayed in Figure 4A. The nucleic acid **13** consisting of the anti-ATP aptamer sequence (domain III) and conjugated to the nucleic-acid-protected red-emitting luminescent AgNCs acted as functional probe to analyze ATP. Similarly, the nucleic acid **14** composed of the anti-ATP aptamer sequence (domain III), conjugated to the nucleic acid sequence protecting the near-infrared-emitting AgNCs, was used as functional probe to analyze ATP. The **13**- or **14**-stabilized AgNCs were adsorbed onto GO to yield the quenched AgNCs. In the presence of ATP, the resulting ATP−aptamer complex is desorbed from GO, leading to the luminescence of the respective AgNCs. Figure 4B depicts the fluorescence spectra observed upon analyzing different concentrations of ATP by the red-emitting AgNCs using the **13**−AgNCs-modified GO as sensor matrix. As the concentration of ATP increases, the resulting fluorescence is intensified, consistent with the enhanced desorption of **13**−AgNCs from GO. The method enabled us to detect ATP with a detection limit of 2.5 μM. The analysis of ATP is specific, and the **13**-modified GO does not respond to other nucleotides, Figure 4C. (For the analysis of ATP by the near-infrared-emitting **14**−AgNCs probe associated with GO, see Figure S10, Supporting Information.)

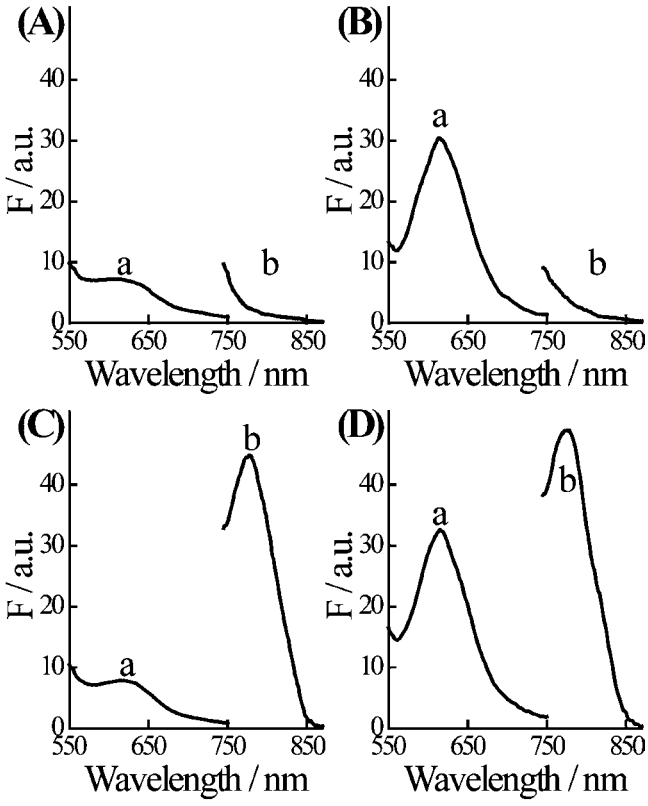

Figure 3. Fluorescence spectra of the AgNCs illustrated in Scheme 2: (A) in the absence of the target genes; (B) in the presence of HIV gene (**8**) and in the absence of HBV gene (**5**); (C) in the presence of HBV gene (**5**) and in the absence of HIV gene (**8**); (D) in the presence of HIV gene (**8**) and HBV gene (**5**). Curves a and b correspond to fluorescence of the red-emitting and the near-infrared-emitting AgNCs, respectively. Fluorescence spectra were recorded after a fixed time interval of 80 min.

The AgNCs fluorescent labels were further implemented for the optical detection of thrombin, Scheme 3. The nucleic acid sequence **15** that includes the antithrombin aptamer sequence (domain IV), separated by a random AT base spacer from the red-emitting nucleic acid sequence (domain I) stabilizing the AgNCs, was adsorbed on GO, and it acted as optical label for the detection of thrombin. Desorption of the probe upon formation of the probe−thrombin aptamer complex leads to the recovery of fluorescence. Figure 5A depicts the time-dependent fluorescence changes upon analyzing thrombin (75 nM) by the **15**−AgNCs-functionalized GO. The desorption process reaches an equilibrium value after ca. 40 min. Figure 5B shows the fluorescence spectra observed upon analyzing different concentration of thrombin by the **15**−AgNCs-functionalized GO for a fixed time-interval of 40 min. As the concentration of thrombin increases, the resulting fluorescence is intensified, consistent with the formation of a higher concentration of the desorbed **15**−AgNCs−thrombin complex. The calibration curve is shown in Supporting Information, Figure S11. The method enables the analysis of thrombin with a detection limit that corresponds to 0.5 nM. It should be noted that within the optimization of the system we discovered that the linkage of the thrombin aptamer chain to the optical AgNCs probe has a critical effect on the performance of the

dx.doi.org/10.1021/ja403485r | J. Am. Chem. Soc. 2013, 135, 11832−11839

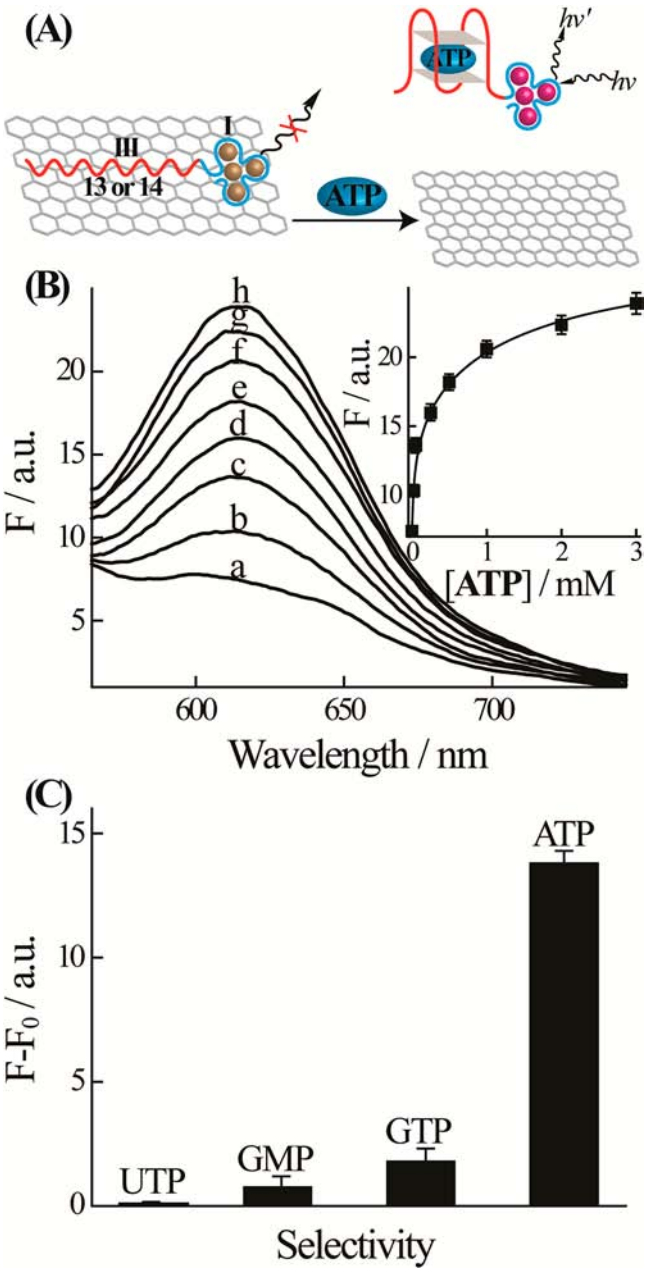

Figure 4. (A) Assay of ATP using DNA-protected aptamer–AgNCs/GO system. (B) Fluorescence spectra of the red-emitting AgNCs upon analyzing different concentrations of ATP by the **13**–AgNCs/GO system: (a) 0, (b) 0.025 mM, (c) 0.05 mM, (d) 0.25 mM, (e) 0.5 mM, (f) 1 mM, (g) 2 mM, and (h) 3 mM. Fluorescence spectra were recorded after a fixed time interval of 60 min. Inset: calibration curve corresponding to the luminescence signal at λ = 616 nm. Error bars were derived from N = 3 experiments. (C) Selectivity of the ATP aptasensor by using 1 mM of UTP, GMP, GTP, and ATP.

sensing device. We find that the direct tethering of the aptamer sequence domain to the nucleic acid functionalized AgNCs, without using the separating AT base spacer, sequence **16**, yields an inefficient probe that is not effectively desorbed from the GO matrix. The time-dependent desorption of the luminescent probes **15**–AgNCs and **16**–AgNCs by thrombin are depicted in Figure 5C, curves a and b, respectively. Although, at present, we do not have a solid explanation for the improved analytical performance of the AT-bridged probe **15**, the results imply that the structural modification of the bridge

Scheme 3. Analysis of Thrombin Using Aptamer–Elongated Nucleic Acid/AgNCs/GO Hybrid System

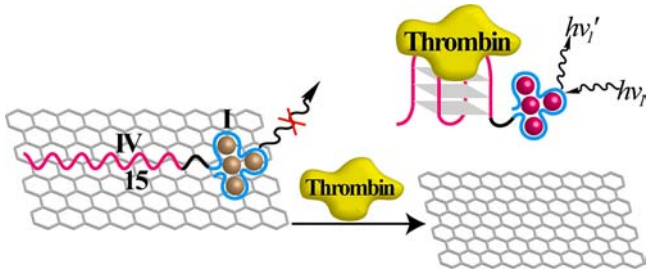

Table 1. Optical DNA and Aptamer–Substrate Complex Sensing Platforms

method/system	detection limit/nM	detection time interval/h	ref
	DNA		
fluorescence, GO/molecular beacon	2	2	13a
fluorescence, releasing acridine orange from reduced GO	50	-	13c
fluorescence, Exo III-assisted target recycling	0.005	1.5	15[a]
fluorescence, autonomous DNAzyme machine	0.01	2.5–3	20a[a]
fluorescence, polymerization/nicking DNA machine	1–10	4–10	20b[a]
fluorescence, GO/nucleic-acid-stabilized AgNCs	0.5	1–1.5	present study
	ATP		
fluorescence, quenching of released dye from dsDNA by GO	0.45–3	2	21a
colorimetric, G-quadruplex DNAzyme	1–10	3	21b
fluorescence, Exo III-assisted analyte recycling	0.25	1–1.5	21c[a]
fluorescence, aptazyme-coupled rolling circle amplification	1	-	21d[a]
fluorescence, GO/nucleic-acid-stabilized AgNCs	2.5	1	present study
	Thrombin		
colorimetric, G-quadruplex DNAzyme	20	5	22a
fluorescence, Exo III-assisted analyte recycling	0.09	1–1.5	21c[a]
fluorescence, polymerization/nicking DNA machine	62.5	2	22b[a]
fluorescence, GO/nucleic-acid-stabilized AgNCs	0.5	0.5–1	present study

[a]Amplified detection.

linking the aptamer sequence to the AgNCs label might be an important parameter for optimizing the sensor performance.

The AgNCs provide an effective luminescence probe for the analysis of DNA or aptamer–substrate complexes. Comparison of the performance of these AgNCs/GO sensing platforms to other optical sensing methods, or GO-based platforms, for sensing DNA or the aptamer substrates ATP and thrombin is important. Table 1 compares different optical methods for analyzing DNA and ATP or thrombin (through aptamers) to the sensing results reported in the present study (for more examples, see Table S2). For analyzing DNA, the GO/AgNCs–nucleic-acid-functionalized matrix reveals better, or comparable, sensing

dx.doi.org/10.1021/ja403485r | J. Am. Chem. Soc. 2013, 135, 11832–11839

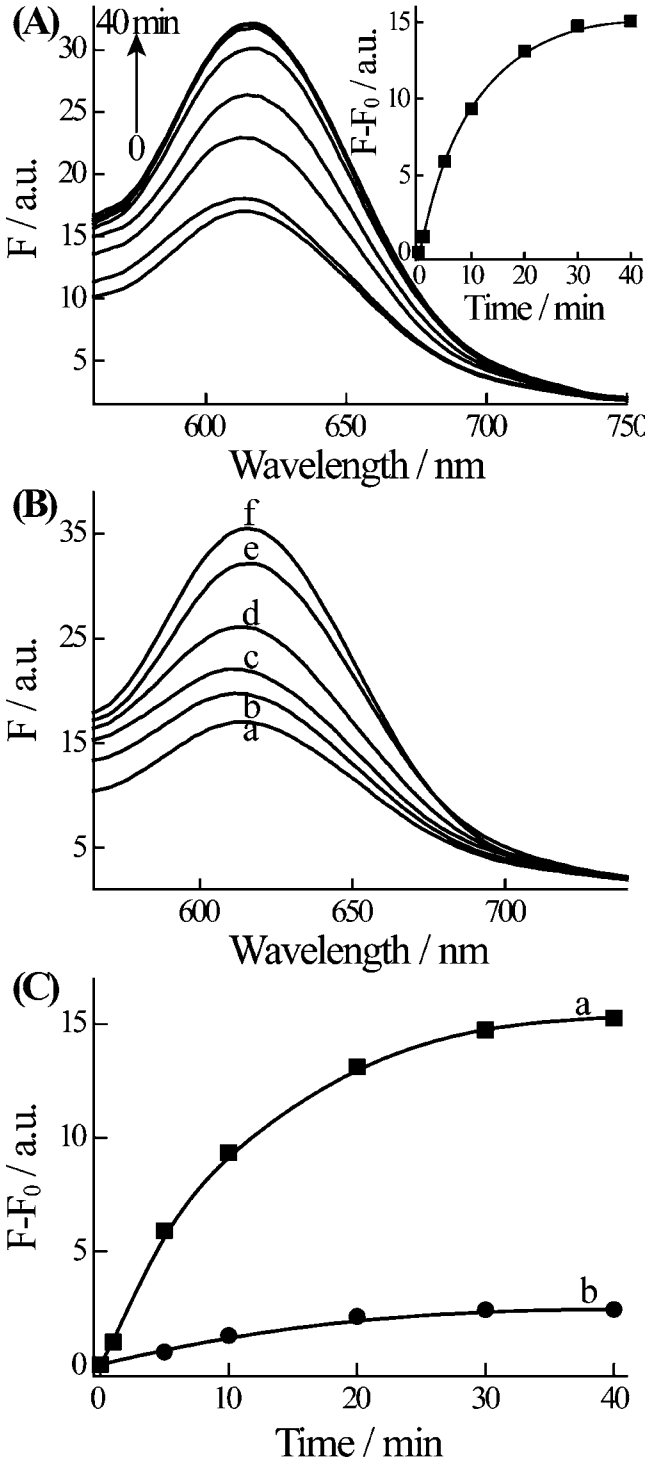

Figure 5. (A) Time-dependent fluorescence spectra changes upon analyzing thrombin (75 nM) by the **15**-functionalized GO. Inset: calibration curve corresponding to the luminescence signal at λ = 616 nm. F_0 and F correspond to the fluorescence of the system in the absence and presence of thrombin, respectively. (B) Fluorescence spectra of the red-emitting AgNCs upon analyzing different concentrations of thrombin by the **15**-functionalized GO: (a) 0, (b) 5 nM, (c) 25 nM, (d) 50 nM, (e) 75 nM, and (f) 100 nM. Fluorescence spectra were recorded after a fixed time interval of 40 min. (C) Time-dependent fluorescence changes upon analyzing 75 nM thrombin by (a) **15**-functionalized GO or (b) **16**-functionalized GO.

performance as compared to other "static" detection methods. Only in the presence of catalytic amplification cycles (e.g., Exo III or DNAzyme) are the sensitivities higher. Nevertheless, these improved sensitivities are accompanied by the moderate stabilities of the enzymes, their cost, and the longer time intervals for analysis. Similarly, for the analysis of ATP or thrombin by the respective aptamers, the AgNCs–aptamer/GO matrices reveal better, or comparable, sensitivities, and the analysis response times of our systems are better when compared to those of other static sensing systems. Only catalytically amplified platforms involving enzymes (e.g., polymerase or Exo III) reveal slightly improved sensitivities. These systems suffer, however, from the need of costly and moderate stability of the biocatalysts.

■ CONCLUSIONS

The present study has introduced the hybrid material consisting of nucleic-acid-stabilized AgNCs and GO as a composite functional matrix for the fluorescence detection of DNA or aptamer–substrate complexes. Two sequence-specific-stabilized AgNCs were implemented in our study: one type included red-emitting (616 nm), DNA-protected AgNCs and the second type involved near-infrared-emitting (775 nm), DNA protected AgNCs. Whereas the DNA-protected AgNCs showed weak affinity for binding to GO, the conjugation of single-stranded nucleic acid tethers to the DNA-protected AgNCs led to efficient adsorption of the nucleic-acid-modified AgNCs to GO, resulting in the effective quenching of the fluorescence of the AgNCs. By the conjugation of nucleic acid sequences that act as recognition probes for target DNAs or as aptamers to the DNA-protected AgNCs, functional nanostructures for the analysis of DNA or aptamer–substrate complexes were tailored. The deposition of the nucleic-acid-functionalized AgNCs onto GO resulted in the fluorescence quenching of the AgNCs. In the presence of the target DNAs, complementary to the single-stranded probe sequences associated with GO, desorption of the duplex DNA structures linked to the AgNCs labels from GO led to the generation of fluorescence as readout signal for the sensing event. By applying the appropriate probe sequences, we analyzed the HBV, the HIV, and the syphilis (*T. pallidum*) genes. The sensing platform revealed selectivity, and a single base mismatch could be discriminated from the target analyte genes. Similarly, the aptamer sequences conjugated to the AgNCs labels were implemented for analyzing the respective substrates, e.g., ATP or thrombin. The anti-ATP aptamer sequence linked to the AgNCs labels revealed selectivity, and other nucleotides, e.g., UTP, GMP, GTP did not desorb the aptamer-modified AgNCs from GO.

Besides the basic scientific interest in AgNCs as a new luminescent optical label for sensing applications and the need to address fundamental questions, such as the rate of release from GO, it is important to discuss the advantages of the AgNCs nucleic acid labels as compared to other luminescent labels (organic fluorophores, quantum dots) and to highlight the potential future perspectives of these materials. (i) The stabilization of different sized AgNCs by sequence-specific oligonucleotides and the formation of tunable luminescent labels provide easy means to tether the label to any DNA or aptamer sensing probe. (ii) The photostability and luminescence brightness reveal substantial advantages over organic fluorophores undergoing photodegradation. (iii) The small sizes of the AgNCs, as compared to molecular fluorophores or semiconductor quantum dots, and their nontoxic features[3] provide versatile means to apply these materials in intracellular media. (iv) The size- and sequence-controlled luminescence

features of the AgNCs and the availability of other fluorescent metal nanoclusters, e.g., AuNCs, provide a new method to fabricate in conjunction with GO optical barcodes for the multiplexed analysis of DNA or aptamer−substrate complexes.

■ ASSOCIATED CONTENT

Ⓢ Supporting Information

Excitation and emission spectra of the AgNCs, fluorescence quenching of the nucleic-acid-protected AgNCs by GO, assay of a random sequence **4** by AgNCs/GO systems, florescence spectra of AgNCs stabilized by **6** in the presence of HBV target gene and in the absence of GO, target analysis of DNA mutation by the nucleic acid−AgNCs/GO system and stringency control experiment, assay of the HIV gene using the red-emitting AgNCs, assay of the HBV gene using the near-infrared-emitting AgNCs, optimization of synthetic conditions for target detection, multiplexed detection of HBV gene and syphilis gene, assay of ATP using the near-infrared-emitting AgNCs, calibration curve for the assay of thrombin, comparison of different platforms for the analysis of target DNA, ATP and thrombin. This material is available free of charge via the Internet at http://pubs.acs.org.

■ AUTHOR INFORMATION

Corresponding Author

willnea@vms.huji.ac.il

Notes

The authors declare no competing financial interest.

■ ACKNOWLEDGMENTS

Parts of this research are supported by the NanoSensoMach ERC Grant No. 267574 under the EU FP7/2007-2013 program and by the Israel National Nanotechnology Initiative (INNI), Focal Technology Areas program.

■ REFERENCES

(1) (a) Gwinn, E. G.; O'Neill, P.; Guerrero, A. J.; Bouwmeester, D.; Fygenson, D. K. *Adv. Mater.* **2008**, *20*, 279−283. (b) Richards, C. I.; Choi, S.; Hsiang, J. C.; Antoku, Y.; Vosch, T.; Bongiorno, A.; Tzeng, Y. L.; Dickson, R. M. *J. Am. Chem. Soc.* **2008**, *130*, 5038−5039.

(2) (a) Sharma, J.; Rocha, R. C.; Phipps, M. L.; Yeh, H.; Balatsky, K. A.; Vu, D. M.; Shreve, A. P.; Werner, J. H.; Martinez, J. S. *Nanoscale* **2012**, *4*, 4107−4110. (b) Petty, J. T.; Fan, C.; Story, S. P.; Sengupta, B.; Sartin, M.; Hsiang, J.-C.; Perry, J. W.; Dickson, R. M. *J. Phys. Chem. B* **2011**, *115*, 7996−8003. (c) Petty, J. T.; Fan, C.; Story, S. P.; Sengupta, B.; Iyer, A. S.; Prudowsky, Z.; Dickson, R. M. *J. Phys. Chem. Lett.* **2010**, *1*, 2524−2529. (d) O'Neill, P. R.; Velazquez, L. R.; Dunn, D. G.; Gwinn, E. G.; Fygenson, D. K. *J. Phys. Chem. C* **2009**, *113*, 4229−4233.

(3) (a) Choi, S.; Dickson, R. M.; Yu, J. *Chem. Soc. Rev.* **2012**, *41*, 1867−1891. (b) Han, B.; Wang, E. *Anal. Bioanal. Chem.* **2012**, *402*, 129−138. (c) Latorre, A.; Somoza, Á. *ChemBioChem* **2012**, *13*, 951−958.

(4) Su, Y.-T.; Lan, G.-Y.; Chen, W.-Y.; Chang, H.-T. *Anal. Chem.* **2010**, *82*, 8566−8572.

(5) Chen, W.-Y.; Lan, G.-Y.; Chang, H.-T. *Anal. Chem.* **2011**, *83*, 9450−9455.

(6) Liu, X.; Wang, F.; Niazov-Elkan, A.; Guo, W.; Willner, I. *Nano Lett.* **2013**, *13*, 309−314.

(7) (a) Zhang, L.; Zhu, J.; Guo, S.; Li, T.; Li, J.; Wang, E. *J. Am. Chem. Soc.* **2013**, *135*, 2403−2406. (b) Sharma, J.; Yeh, H.-C.; Yoo, H.; Werner, J. H.; Martinez, J. S. *Chem. Commun.* **2011**, *47*, 2294−2296. (c) Li, J.; Zhong, X.; Zhang, H.; Le, X. C.; Zhu, J.-J. *Anal. Chem.* **2012**, *84*, 5170−5174.

(8) (a) Yeh, H.-C.; Sharma, J.; Han, J. J.; Martinez, J. S.; Werner, J. H. *Nano Lett.* **2010**, *10*, 3106−3110. (b) Yeh, H.-C.; Sharma, J.; Shih, I.-M.; Vu, D. M.; Martinez, J. S.; Werner, J. H. *J. Am. Chem. Soc.* **2012**, *134*, 11550−11558.

(9) Shah, P.; Rørvig-Lund, A.; Chaabane, S. B.; Thulstrup, P. W.; Kjaergaard, H. G.; Fron, E.; Hofkens, J.; Yang, S. W.; Vosch, T. *ACS Nano* **2012**, *6*, 8803−8814.

(10) Li, J.; Zhong, X.; Cheng, F.; Zhang, J.-R.; Jiang, L.-P.; Zhu, J.-J. *Anal. Chem.* **2012**, *84*, 4140−4146.

(11) (a) Erickson, K.; Erni, R.; Lee, Z.; Alem, N.; Gannett, W.; Zettl, A. *Adv. Mater.* **2010**, *22*, 4467−4472. (b) Morales-Narváez, E.; Merkoçi, A. *Adv. Mater.* **2012**, *24*, 3298−3308.

(12) Loh, K. P.; Bao, Q.; Eda, G.; Chhowalla, M. *Nat. Chem.* **2010**, *2*, 1015−1024.

(13) (a) Lu, C.-H.; Li, J.; Liu, J.-J.; Yang, H.-H.; Chen, X.; Chen, G.-N. *Chem. Eur. J.* **2010**, *16*, 4889−4894. (b) Jang, H.; Ryoo, S. R.; Kim, Y. K.; Yoon, S.; Kim, H.; Han, S. W.; Choi, B. S.; Kim, D. E.; Min, D. H. *Angew. Chem., Int. Ed.* **2013**, *52*, 2340−2344. (c) Shi, Y.; Tao, W.; Huang, H. Q.; Luo, N.; Li, B. *Chem. Commun.* **2011**, *47*, 4676−4678.

(14) Lu, C.-H.; Yang, H.-H.; Zhu, C.-L.; Chen, X.; Chen, G.-N. *Angew. Chem., Int. Ed.* **2009**, *48*, 4785−4787.

(15) Liu, X.; Aizen, R.; Freeman, R.; Yehezkeli, O.; Willner, I. *ACS Nano* **2012**, *6*, 3553−3563.

(16) (a) Li, Y.; Cu, Y. T. H.; Luo, D. *Nat. Biotechnol.* **2005**, *23*, 885−889. (b) Choi, H. M.; Chang, J. Y.; Trinh, L. A.; Padilla, J. E.; Frase, S. E.; Pierce, N. A. *Nat. Biotechnol.* **2010**, *28*, 1208−1212.

(17) (a) Song, F.; Tang, P. S.; Durst, H.; Cramb, D. T.; Chan, W. C. W. *Angew. Chem., Int. Ed.* **2012**, *51*, 8773−8777. (b) Algar, W. R.; Krull, U. J. *Anal. Bioanal. Chem.* **2010**, *398*, 2439−2449. (c) Freeman, R.; Liu, X.; Willner, I. *Nano Lett.* **2011**, *11*, 4456−4461. (d) Geißler, D.; Stufler, S.; Löhmannsröben, H.-G.; Hildebrandt, N. *J. Am. Chem. Soc.* **2013**, *135*, 1102−1109.

(18) (a) Stoeva, S. I.; Lee, J.-S.; Thaxton, C. S.; Mirkin, C. A. *Angew. Chem., Int. Ed.* **2006**, *45*, 3303−3306. (b) Nicewarner-Peña, S. R.; Freeman, R. G.; Reiss, B. D.; He, L.; Pena, D. J.; Walton, I. D.; Cromer, R.; Keating, C. D.; Natan, M. J. *Science* **2001**, *294*, 137−141.

(19) (a) Hummers, W. S.; Offeman, R. E. *J. Am. Chem. Soc.* **1958**, *80*, 1339. (b) Marcano, D. C.; Kosynkin, D. M.; Berlin, J. B.; Sinitskii, A.; Sun, Z.; Slesarev, A.; Alemany, L. B.; Lu, W.; Tour, J. M. *ACS Nano* **2010**, *8*, 4806−4814.

(20) (a) Wang, F.; Elbaz, J.; Willner, I. *J. Am. Chem. Soc.* **2012**, *134*, 5504−55007. (b) Orbach, R.; Mostinski, L.; Wang, F.; Willner, I. *Chem. Eur. J.* **2012**, *18*, 14689−14694.

(21) (a) Pu, W. D.; Zhang, L.; Huang, C. Z. *Anal. Methods* **2012**, *4*, 1662−1666. (b) Liu, X.; Freeman, R.; Golub, E.; Willner, I. *ACS Nano* **2011**, *5*, 7648−7655. (c) Liu, X.; Freeman, R.; Willner, I. *Chem. Eur. J.* **2012**, *18*, 2207−2211. (d) Cho, E. J.; Yang, L.; Levy, M.; Ellington, A. D. *J. Am. Chem. Soc.* **2005**, *127*, 2022−2023.

(22) (a) Li, T.; Wang, E.; Dong, S. *Chem. Commun.* **2008**, 3654−3656. (b) Zhu, C.; Wen, Y.; Li, D.; Wang, L.; Song, S.; Fan, C.; Willner, I. *Chem. Eur. J.* **2009**, *15*, 11898−11903.